

Anisotropic diffusion of 3d metals on W(110): Competition between crystalline structure and surface steps

D. Reuter, G. Gerth, and J. Kirschner

Max-Planck-Institut für Mikrostrukturphysik, Weinberg 2, D-06120, Germany

(Received 29 August 1997)

A dot of Fe, Co, Ni, or Cu was deposited on a clean W(110) surface by evaporation through a mask (\varnothing 100 μm). Upon annealing at 720–1070 K we observed by scanning Auger microscopy that for Fe, Co, and Ni a 1-ML-thick film spreads across the surface, whereas for Cu the simultaneous spreading of 1 and 2 ML was found. For all materials the spreading is anisotropic, though significant differences between the elements were found. For Fe the fast spreading direction is along $\langle 110 \rangle$ and the anisotropy is caused by the crystallographic structure of the substrate. For Co and Ni the fast spreading direction is determined at low spreading temperatures (≤ 820 K) by the steps on the substrate surface. For the higher spreading temperatures the influence of the steps becomes weaker and the crystallographic structure tends to determine the spreading anisotropy. For Cu, the fast spreading direction for the first ML is along the step direction whereas the crystallographic structure causes an anisotropic spreading of the second ML. The spreading behavior is discussed within the “unrolling carpet” model. [S0163-1829(98)02804-5]

I. INTRODUCTION

Surface diffusion plays an important role in many fields of surface science, e.g., in heterogeneous catalysis or the growth of thin films. This has motivated numerous studies in the past^{1–5} using various experimental approaches. These approaches can be roughly divided in two classes: On the one hand, the random walk of a single atom in the absence of a concentration gradient is studied whereas in the so-called “spreading experiments,” where the spreading of material from a “source” region on the surface is investigated, the motion of many atoms under the influence of a concentration gradient is studied. The experiments we present in this paper belong to the second class.

Our study of the spreading behavior of Fe, Co, Ni, and Cu on W(110) were motivated by two main reasons. Firstly, the magnetic properties of ultrathin ferromagnetic films on single-crystal surfaces are an intensively studied subject. It has been shown that the magnetic properties of these films are often correlated with their morphology. A good example for this correlation is the system Fe/W(110).⁶ As thin films grow mostly far away from thermal equilibrium, the morphology is often determined by the mobility of the adsorbing atoms. Therefore, the understanding of surface diffusion on an atomic scale is important for a better understanding of film growth. Spreading experiments on a micrometer scale can give indirect information on the underlying atomic processes. Secondly, the preparation of laterally structured magnetic films has drawn much attention in the past.⁷ The temperature stability of these microstructures is an important question, with respect to their possible technical applications. Spreading experiments like ours may give directly valuable information on diffusion processes at high temperature. In addition, Fe, Co, Ni, and Cu on W(110) may also serve as model systems for studying surface diffusion because even at elevated temperatures there is no alloy formation between film and substrate nor diffusion of the adsorbate atoms into

the bulk of the substrate.^{6,8–12} Therefore the spreading behavior is completely determined by surface diffusion.

In our experiments we generated the source region on the surface by evaporating through a mask with a hole (\varnothing 100 μm), which resulted in a circular dot. There are two interesting questions we wanted to answer with our experiments: Which concentration profile evolves during annealing of the sample, and is the spreading isotropic? The dot represents a rectangular starting concentration profile and if the diffusion coefficient D is independent of the concentration c a Gaussian concentration profile after annealing is predicted by the diffusion equation.¹³ For surface diffusion the assumption that D is independent of c is in most cases not valid^{14,15} and deviations from a Gaussian concentration profile are observed. In some cases even a film of constant thickness spreads across the surface (“unrolling carpet”).¹⁶ The concentration dependence of D is due to adsorbate-substrate and adsorbate-adsorbate interactions.¹⁶ So far two reasons for anisotropic spreading have been reported. One is the crystallographic structure of the substrate,¹⁷ i.e., twofold symmetry of the surface, and the other reason is steps on the surface,¹⁸ i.e., fast spreading along the step direction. For the W(110) surface both kinds of anisotropic spreading could be expected because of the twofold symmetry of the surface. Indeed, we observe step-dominated anisotropic spreading as well as anisotropies caused by the crystallographic structure. Which of the two regimes dominates depends on material and temperature.

II. EXPERIMENTAL ASPECTS

All experiments were performed in a Physical Electronics SAN 670 xi Auger microscope with a base pressure below 1×10^{-10} mbar. By putting a mask with a hole close (distance about 100 μm) to the crystal surface and depositing metal vapor through it we prepared a dot with a diameter of approximately 100 μm on the clean surface. The dots could be prepared at the desired position on the surface with an

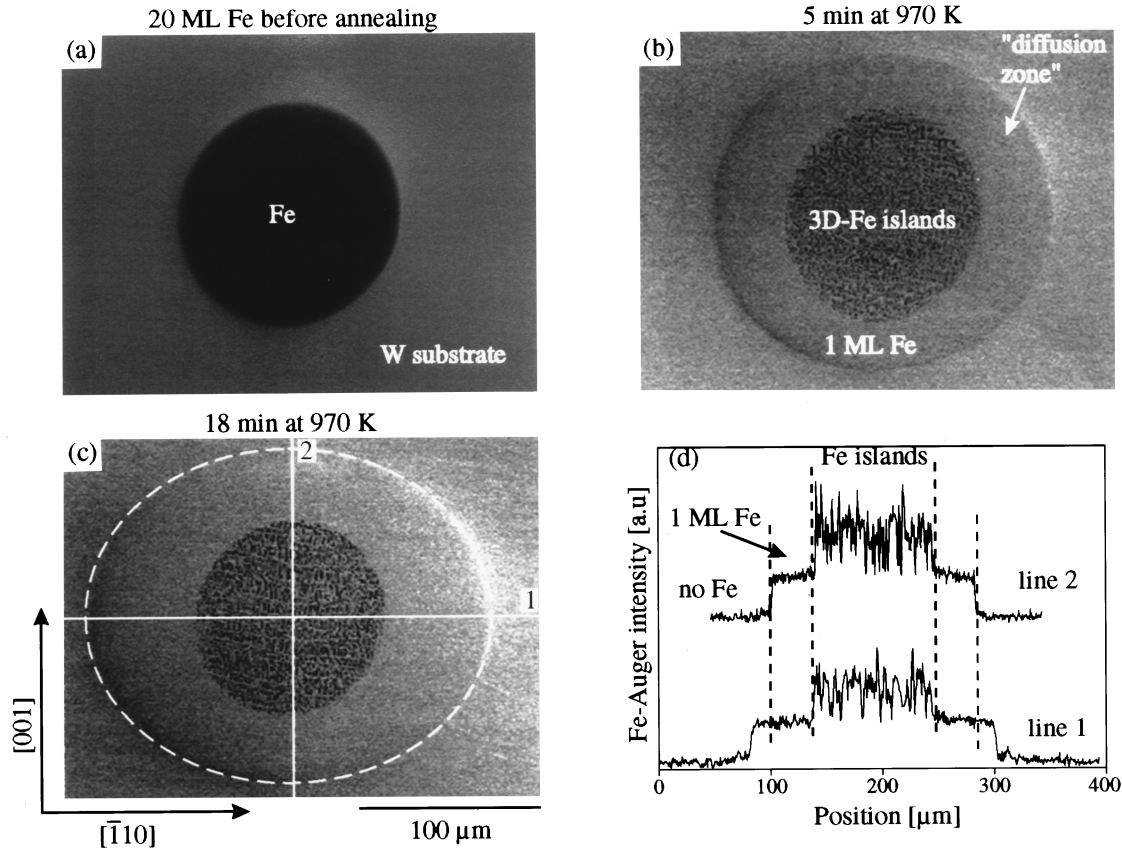


FIG. 1. Spreading of Fe from a 20 ML Fe dot. In (a)–(c) secondary electron images are shown. The anisotropic spreading can be seen in (b) and (c). Auger line profiles along the lines depicted in (c) are shown in (d). In these profiles the intensity of the Fe(703 eV)-Auger transition was measured. It is clearly seen that the Fe-Auger intensity is constant in the diffusion zone. The intensity in the diffusion zone corresponds to a Fe coverage of 1 ML. The large intensity variations in the central part of the profiles reflect the island structure in the central part of the original dot area.

accuracy of $\pm 100 \mu\text{m}$. After preparing the dot, we analyzed it by scanning electron and scanning Auger microscopy (SEM and SAM). Then we annealed the sample repeatedly for 20 s to 30 min at temperatures between 720 and 1070 K and analyzed the dot in between.

The Fe, Co, and Ni were evaporated from high-purity materials using an electron-beam evaporator whereas Cu was deposited from a W 25% Re wire basket, which was resistively heated. The thickness of the deposit was checked with a quartz microbalance. During evaporation the pressure was below 2×10^{-10} mbar. The cleanliness of the deposited material was checked with Auger electron spectroscopy (AES). For all metals the contamination level was below the detection limit.

The tungsten crystal was oriented with a deviation less than 0.4° from (110). The sample was heated by electron bombardment and the temperature was measured using a W-W 26% Re thermocouple. The crystal was cleaned by cycles of annealing at 1800 K in 1×10^{-7} mbar oxygen and a subsequent flash to 2300 K. The impurity concentration was controlled by AES and was found to be below 3% of an atomic layer.

III. RESULTS

Figures 1(a)–(c) show an annealing sequence at 970 K for a 20-ML-thick Fe dot. Two significant changes are observed

after 5 min at 970 K as can be seen in Fig. 1(b). One is the formation of large three-dimensional islands inside the original dot area and the other is the spreading of Fe across the tungsten surface. The islands have an elongated shape and are oriented predominantly along the $\langle 100 \rangle$ direction of the substrate surface as secondary electron images (SE images) with higher magnification show. We conclude from laterally resolved Auger electron spectroscopy that the islands are more than 30 ML high with 1 ML Fe covering the tungsten substrate between them. The formation of three-dimensional islands with one thermally stable ML upon annealing was already proposed by Berlowitz and co-workers⁸ to explain their experimental results. In this paper we will not discuss the island formation but focus on the spreading behavior. Throughout this paper we will call the area covered by the spreading material the “diffusion zone.”

Figure 1(c) shows clearly that after annealing at 970 K for 18 min the diffusion zone is elliptically shaped with the long axis along the $\langle 110 \rangle$ directions of the W(110) surface. This means that the Fe spreading is anisotropic with the fast spreading direction along $\langle 110 \rangle$ and the slow spreading direction along $\langle 100 \rangle$. After annealing for 5 min at the same temperature [Fig. 1(b)] the diffusion zone is also elliptically shaped although not as pronouncedly as in Fig. 1(c). For Fe the shape of the diffusion zone depends neither on the dot position on the substrate nor on the annealing temperature. Co, Ni, and Cu behave differently, as shown below.

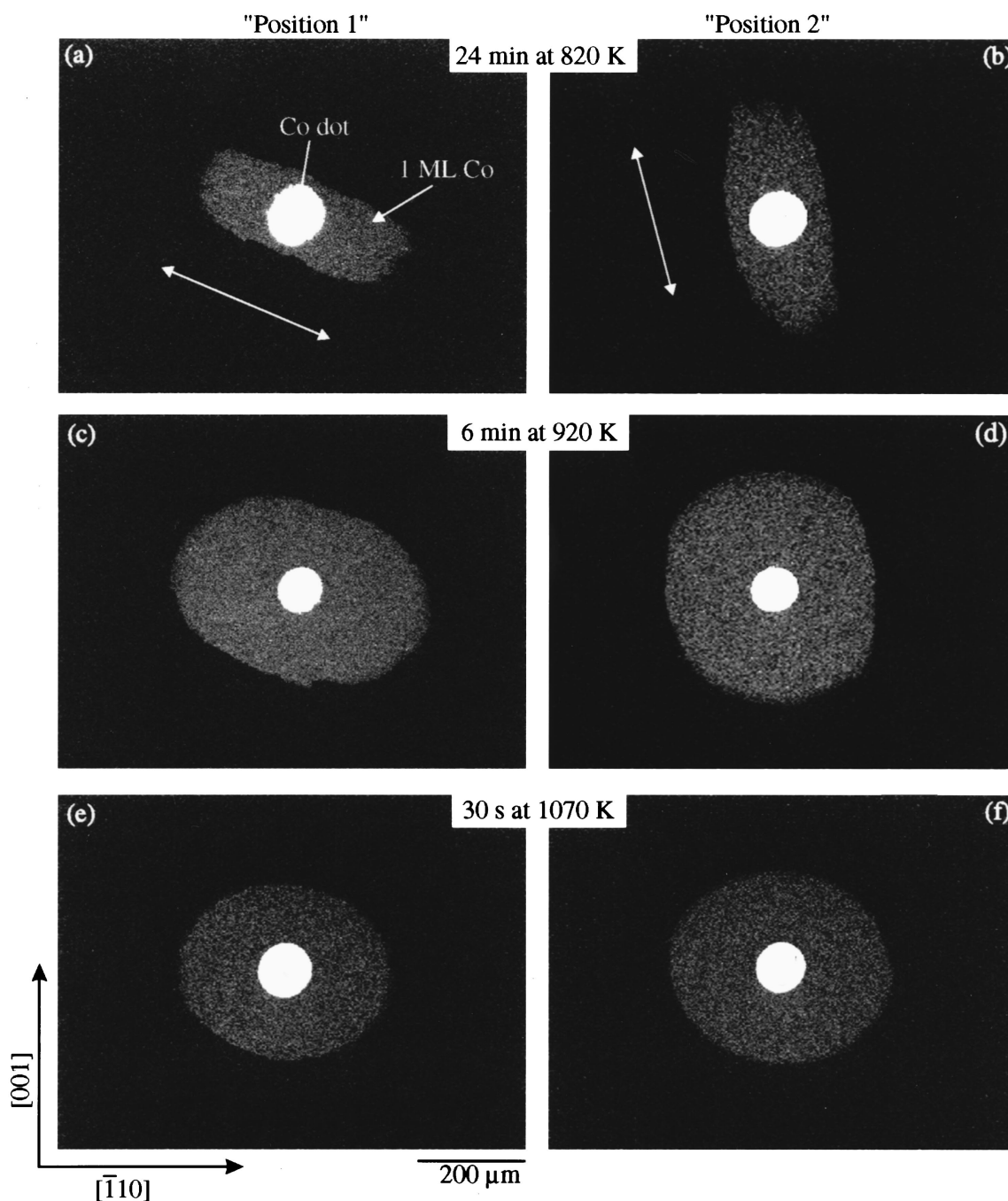


FIG. 2. Spreading of Co at two different positions on the W(110) surface and at various temperatures. The Auger maps show the lateral intensity distribution for the Co(775 eV)-Auger transition. The Co coverage in the diffusion zone is 1 ML. From the differences in the spreading anisotropies for the two positions one can conclude on the influence of steps on the spreading, as discussed in detail in the text. The white arrows indicate the supposed step direction for each of the two positions on the surface. The thickness of the Co dot was initially 20 ML.

In Fig. 1(d) Fe-Auger line profiles along the $\langle 110 \rangle$ and the $\langle 100 \rangle$ directions are shown, respectively. These line profiles show a constant Fe signal intensity within the diffusion zone with a sharp drop to zero at the edge of the diffusion zone. This means that the Fe concentration is constant in the diffusion zone. The Fe signal intensity in the diffusion zone corresponds to 1 ± 0.1 ML as we conclude from the comparison of the W(169 eV) Auger signal intensity from within the diffusion zone and from the uncovered surface. This concentration profile was observed independent of the dot position

on the surface and throughout the entire temperature range investigated (870–1070 K). The strong intensity variations in the central part of the dot area reflect the island structure inside the original dot area as seen in the SE images.

The spreading of Co for various temperatures at two different positions on the tungsten surface is shown in Fig. 2. The Auger maps of Figs. 2(a), 2(c), and 2(e) were taken at the same position on the W crystal surface. This position we will refer to throughout this paper as “position 1.” The position where the Auger maps shown in Figs. 2(b), 2(d), and

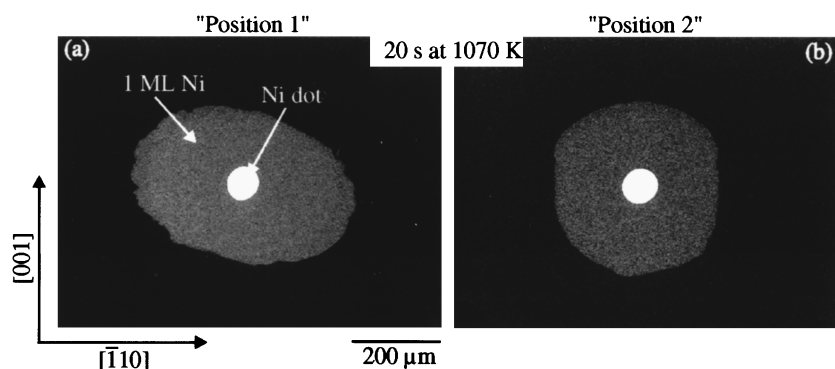


FIG. 3. Spreading of Ni at 1070 K at two different positions on the W(110) surface. The Auger maps show the lateral intensity distribution for the Ni(775 eV)-Auger transition. The thickness of the Ni dot was initially 20 ML. It is clearly seen from the different shaped diffusion zones for the two positions that there is a strong influence of the steps on the spreading anisotropy.

2(f) were taken will be referred to as “position 2.” It was located approximately 2 mm away from position 1. Independent of dot position and throughout the entire temperature range investigated, we observed the same concentration profile in the diffusion zone for the spreading of Co, i.e., a constant coverage of 1 ML in the diffusion zone with a sharp drop to zero at its edge.

The Co spreading at 820 K is strongly anisotropic for both dot positions as seen in Figs. 2(a) and 2(b) but the fast spreading direction is different at the two positions. At position 1 the fast direction includes an angle of approximately 25° with the $\langle 110 \rangle$ direction whereas the fast spreading direction is almost parallel to $\langle 100 \rangle$ at position 2. For 920 K the spreading anisotropy is not as pronounced as at 820 K [Figs. 2(c) and 2(d)]. It seems that the fast direction is tilted marginally towards the $\langle 110 \rangle$ directions at position 1, while at position 2 the anisotropy is less pronounced than at position 1. Figures 2(e) and 2(f) show that at 1070 K the diffusion zones are nearly identical for both positions. At this temperature the anisotropy is very similar to the anisotropy observed for the spreading of Fe.

For Ni a series of experiments were made similar to those performed for Co. A 1-ML-thick film with a sharp boundary spreads across the surface in complete analogy to Fe and Co. Upon annealing at 820 K the fast spreading direction is the same as for Co with an even stronger anisotropy. At 920 K the anisotropy is less pronounced but the fast spreading di-

rections are the same as for 820 K. At 1070 K the diffusion zones for the Ni spreading (see Fig. 3) for the two positions 1 and 2 look very similar to the diffusion zones for the Co spreading at 920 K [Figs. 2(c) and 2(d)]. The temperature dependence of the spreading anisotropy for Ni is the same as for Co but similarly shaped diffusion zones for Ni and Co spreading are observed at temperatures approximately 150 K higher for Ni than for Co. This means that the temperature induced changes in the spreading anisotropies are shifted to higher temperatures for Ni compared to Co.

In Fig. 4 the development of an 8 ML Cu dot at position 1 for a diffusion temperature of 820 K is shown. In contrast to the metals discussed so far we observed the spreading of two distinct coverages. Line profiles show that the edges of the two zones are sharp and from laterally resolved Auger electron spectroscopy we conclude that the coverages are 1 and 2 ML, respectively. Auger maps with higher magnification show that Cu forms three-dimensional islands in the original dot area. Between the islands, 2 ML Cu cover the W(110) substrate. This island formation with two thermally stable ML was previously reported by Bauer and coworkers.¹² After the original Cu dot is completely dissolved, the size of the area covered by 2 ML starts to decrease whereas the first ML continues spreading. For the first ML the fast spreading direction is along the step direction for the entire temperature range investigated (620 to 820 K). For the second ML the form of the diffusion zone is of course

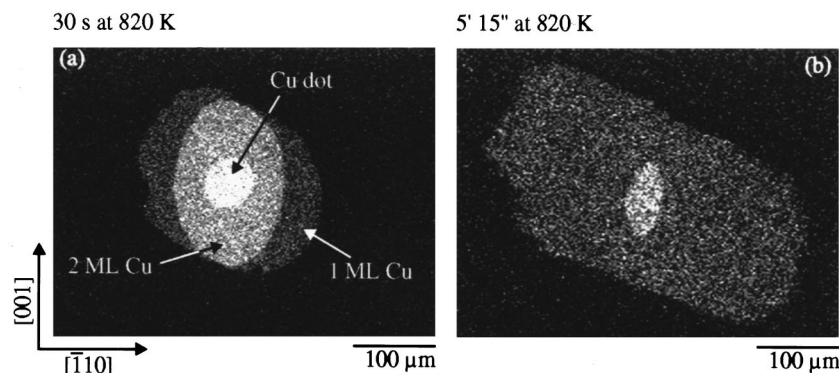


FIG. 4. Spreading behavior of Cu at 820 K. The lateral intensity distribution of the Cu(912 eV)-Auger transition is shown. The thickness of the Cu dot was 8 ML initially. The distinct coverages are indicated in the images. Figure 4(b) shows that the size of the area covered by 2 ML decreases after the original dot is completely dissolved, whereas the first ML continues to spread out. The fast spreading direction for the first ML is along the step direction, whereas the fast spreading for the second ML is along $\langle 100 \rangle$.

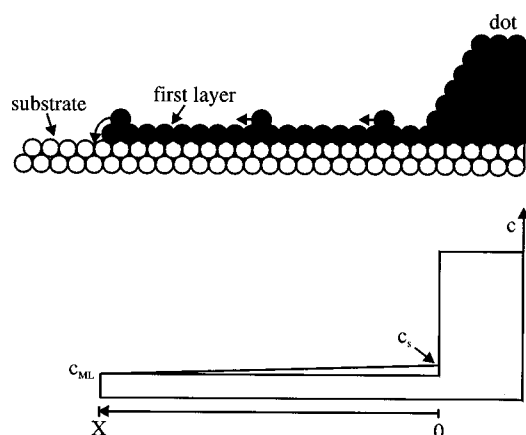


FIG. 5. (a) shows a hard ball model of the "unrolling carpet" mechanism. The concentration on top of the first ML is exaggerated. In (b) the concentration profile used for the quantitative description of the "unrolling carpet" mechanism discussed in the text is shown. The concentration gradient on top of the first ML is exaggerated.

influenced by the spreading anisotropy of the first layer, but if this is the only reason for the elliptically shaped 2 ML zone, the long axis of the ellipse should be perpendicular to the fast spreading direction of the first ML. Figure 4 shows that this is not the case. Instead, the long axis of the ellipse is along $\langle 100 \rangle$. Thus, we can conclude that the fast spreading direction for the second ML is also along $\langle 100 \rangle$.

IV. DISCUSSION

We will first discuss the concentration profiles in the diffusion zone for the four metals investigated. Fe, Co, and Ni show qualitatively the same concentration profiles in the diffusion zone, i.e., a 1-ML-thick film with a sharp boundary spreads across the surface. This spreading behavior has been found for other systems, e.g., Pd on W(110),¹⁶ and is known as "unrolling carpet" behavior.^{16,19} Figure 5(a) shows schematically how the corresponding "unrolling carpet" model describes the propagation of the diffusion zone. It is assumed that the atoms in the first ML are immobile. On top of the first layer, atoms diffuse in a very dilute concentration under the influence of a concentration gradient [Fig. 5(b)]. As soon as they reach the edge of the diffusion zone and come into contact with the substrate they get trapped. This was discussed in detail for the spreading of Pd and Au on W(110) by Butz and Wagner.¹⁶ They supposed a higher binding energy of atoms in the first ML compared to atoms in subsequent layers to be the reason for this kind of spreading behavior. For Fe, Co, and Ni on W(110) this argument also holds as thermal desorption spectroscopy (TDS) reveals. TDS (Refs. 8–11) shows for Fe, Co, and Ni two clearly separated desorption peaks. The peak at the higher temperature is attributed to desorption from the first layer, whereas the peak at the lower temperature is due to desorption of atoms in excess of the first layers. This means that for all three metals the atoms in the first layer have a higher binding energy than atoms in higher layers. This similarity in the binding conditions for Fe, Co, and Ni is reflected in the similarity of the concentration profiles in the diffusion zone.

A different spreading behavior is observed for Cu. Here a

1- and a 2-ML-thick film spread simultaneously across the surface. TDS (Ref. 12) shows three separated desorption peaks for Cu on W(110). This means that atoms in the first ML have the highest binding energy. Atoms in the second ML have a lower binding energy compared to atoms in the first layer but atoms in subsequent layers have an even lower binding energy. This is in contrast to Fe, Co, and Ni on W(110) for which the binding energy for atoms in the second and subsequent layers is the same within the resolution of TDS. Obviously, the influence of the substrate reaches farther into the overlayer of Cu than into Fe, Co, and Ni. Thus, the spreading behavior of Cu on W(110) can be explained by an "unrolling carpet" mechanism both for the propagation of the first and the second ML zone. This means that atoms diffuse on top of the second ML and fall on top of the first ML as soon as they reach the edge of the second ML zone. The atoms either stay at the edge of the second ML zone, which leads to growth of this zone or they diffuse away on top of the first ML and become immobile as soon as they reach the edge of the first ML zone and come into contact with the W substrate. The diffusion on top of the first layer leads to the growth of the 1 ML zone.

Now we will discuss the reasons for the spreading anisotropies for Fe, Co, and Ni. Cu is discussed separately. As mentioned above the diffusion zone propagates in the "unrolling carpet" model via diffusion of atoms on top of the first immobile ML. This means that the crystallographic structure of the first ML can determine the anisotropy. In this case the anisotropy should be independent of the dot position. In our experiments we cannot determine the crystallographic structure in the diffusion zone, and, therefore, rely on assumptions based on experimental data from growth experiments. For Fe (Refs. 6, 8, 20, and 21) the first ML grows pseudomorphically on the W(110) substrate, i.e., it has bcc(110) structure. For Co (Ref. 22) and Ni (Refs. 11, 23, and 24) a transition from a pseudomorphic layer to a distorted fcc(111) structure was observed. TDS (Refs. 23 and 25) shows that for Ni the binding energy is higher in the pseudomorphic layer than in the distorted fcc(111) layer. Because of the similarities in the growth mode we think this is also valid for Co. The concentration in which the atoms have the highest binding energy should spread across the surface.¹⁶ Thus, we assume that the crystallographic structure of Fe, Co, and Ni in the diffusion zone is pseudomorphic to the W(110) surface, i.e., the ML has bcc(110) structure.

We found that for Fe the spreading anisotropy does not depend on the dot position on the surface. Therefore, we conclude that the spreading anisotropy for Fe is only determined by the crystallographic structure in the diffusion zone. Because of the twofold symmetry of a bcc(110) surface an anisotropic spreading is not surprising; details are discussed below. As we assume the same crystallographic structure in the diffusion zone we should observe the same spreading anisotropy for Co and Ni as for Fe. This is only true for Co spreading at high temperatures (1070 K). Only then the crystallographic structure determines the spreading anisotropy. In the other cases the anisotropy depends strongly on the dot position on the surface. This means that the anisotropy depends on the local morphology of the substrate surface. In their work on vicinal W(110) surfaces Butz and Wagner¹⁸ have shown that steps can determine the spreading anisotropy.

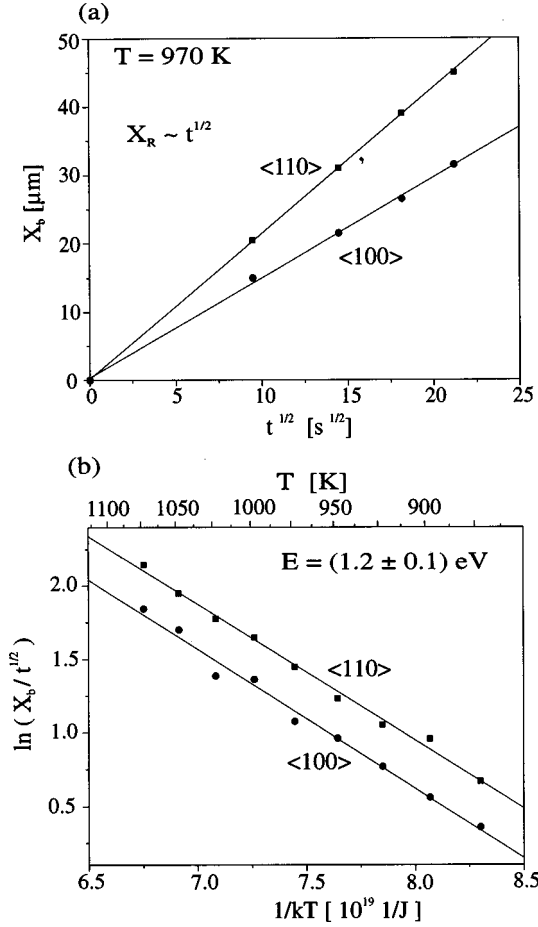


FIG. 6. Quantitative analysis of the spreading of Fe on W(110). (a) shows the time dependence of the spreading length X_b for 970 K. X_b proportional to \sqrt{t} is confirmed for the slow and the fast spreading direction. (b) shows an Arrhenius plot for experiments at various diffusion temperatures T . From the slopes of the straight lines the overall activation energy for the spreading process was determined. One obtains for both spreading directions the same activation energy of 1.2 eV. For all temperatures the spreading length X_b along $\langle 110 \rangle$ is approximately a factor $\sqrt{2}$ larger than along $\langle 100 \rangle$.

ropy and that the fast spreading direction is along the steps. Therefore, we suppose that we have large areas on the surface with preferential step directions. Different step orientations at position 1 and 2 would then explain the different fast spreading directions. The supposed step directions for the two positions are indicated in Figs. 2(a) and 2(b) by white arrows. For higher temperatures, the shapes of the diffusion zones become more similar for the two positions, which means that the influence of steps weakens and the crystallographic structure in the diffusion zone tends to determine the spreading anisotropy. So we conclude that the anisotropy caused by steps is superimposed onto the anisotropy caused by the crystallographic structure in the diffusion zone. We will discuss later by which mechanism steps may influence the spreading behavior.

Now we will discuss quantitatively the Fe spreading for which the anisotropy is determined by the crystallographic structure in the diffusion zone. Butz and Wagner^{16,18} and Noro and co-workers²⁶ developed a quantitative description of the “unrolling carpet” mechanism. The concentration

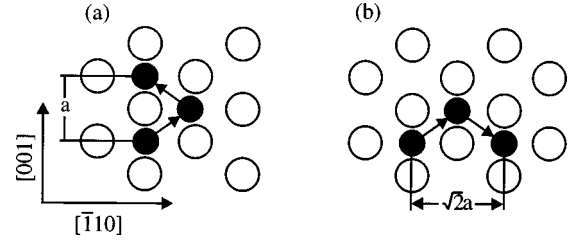


FIG. 7. Single hopping model for diffusion on a bcc(110) surface. The dark circles represent the diffusing atom. The motion of the atom occurs via jumps along the close-packed $\langle 111 \rangle$ directions of the surface. The distance covered along $\langle 110 \rangle$ (b) is $\sqrt{2}$ times larger than the distance covered along $\langle 100 \rangle$ (a). The activation energy for both directions is the same because the motion proceeds for both directions via the same kind of jumps. From these two observations it is clear, that the diffusion coefficient along $\langle 110 \rangle$ for all temperatures is twice that of the diffusion coefficient along $\langle 100 \rangle$. The lattice constant of the substrate is given by a .

profile they used for the calculations is depicted in Fig. 5(b). The diffusion on top of the first ML is described by Fick’s law and the atoms in the first ML are treated as immobile. For a one-dimensional diffusion problem one obtains for the time dependence of the spreading length X_b ,

$$X_b = \sqrt{2D \frac{c_S - c_{ML}}{c_{ML}} t}. \quad (1)$$

In Eq. (1) D is the diffusion coefficient for the diffusion on top of the first layer, c_S the concentration very close to the dot, c_{ML} the concentration in the first layer, and t the diffusion time. Equation (1) means that the spreading length X_b is proportional to the square root of the diffusion time t . For a quantitative analysis of the spreading length in our two-dimensional diffusion problem we exploit only experiments with short diffusion times and, therefore, short spreading lengths, so that we can use Eq. (1) as a good approximation in spite of being rigorously valid only in one dimension. For Fe, Fig. 6(a) shows a plot of the spreading length X_b versus the square root of the diffusion time. A linear dependence is confirmed. For Co the spreading lengths at 1070 K are too big for the one-dimensional approximation of Eq. (1) even for the shortest experimentally feasible diffusion times. For Ni we did not reach the temperature range where the anisotropy is determined by the crystallographic structure before we reach diffusion temperatures where a significant amount of material would evaporate. Therefore, it is not possible to quantitatively discuss the spreading of Co or Ni, respectively, in the regime where the spreading anisotropy is determined by the crystallographic structure.

Both D and $c_S - c_{ML}$ in Eq. (1) are temperature dependent. Obviously the temperature dependence for D should be Arrhenius-like.¹ $c_S - c_{ML}$ is the concentration of atoms on top of the first ML, which is in thermal equilibrium with the source, i.e., the dot. For this concentration we can also expect an Arrhenius-like temperature dependence.^{16,26} With these assumptions for D and $c_S - c_{ML}$ one obtains for the temperature dependence of the spreading length X_b (Refs. 16 and 26),

$$\ln \left(\frac{X_b}{\sqrt{t}} \right) = - \frac{E}{2kT} + \text{const}, \quad E = E_{dT} + E_a. \quad (2)$$

In Eq. (2), E_{dT} is the activation energy for diffusion on top of the first ML, E_a is the difference in binding energy for atoms in the dot and on top of the first ML, k is Boltzmann's constant and T the diffusion temperature. By plotting the logarithmic term in Eq. (2) versus $1/kT$ ("Arrhenius plot"), the overall activation energy for the spreading process can be calculated from the slope of the straight line. This plot is shown for the Fe spreading in Fig. 6(b) for the $\langle 110 \rangle$ and the $\langle 100 \rangle$ directions. The same overall activation energy of (1.2 ± 0.1) eV is obtained. At fixed temperature the ratio of the spreading lengths $X_b^{(110)} : X_b^{(100)}$ lies between 1.3 and 1.5.

We will now present a model that explains the anisotropic spreading with the same activation energies for the fast and the slow spreading direction. Looking at Eq. (1) in principle there are two factors that could be responsible for different spreading lengths in different directions. The diffusion coefficient D and/or the concentration $c_S - c_{ML}$ on top of the first ML could be anisotropic. We will see that it is sufficient to discuss an anisotropic diffusion coefficient D to explain our experimental results. It is known from field ion microscopy²⁷ that single atoms on a bcc(110) surface move via jumps along the closed packed $\langle 111 \rangle$ directions as shown in Fig. 7. The distance covered along the $\langle 110 \rangle$ direction is a factor $\sqrt{2}$ larger than the distance covered along $\langle 100 \rangle$. The activation energy for both directions is the same because the motion in both directions occurs via the same kind of jumps. This means that the diffusion coefficient along $\langle 110 \rangle$ is twice that along $\langle 100 \rangle$ for all temperatures. If this is also true for D in Eq. (1) and $c_S - c_{ML}$ is isotropic, then we should observe the same overall activation energy for both spreading directions and a spreading length that is $\sqrt{2} \approx 1.4$ larger along $\langle 110 \rangle$ than along $\langle 100 \rangle$. This agrees well with our experimental findings as described above.

We will now discuss how steps cause anisotropic spreading. One can imagine two possible ways. On the one hand, the diffusion perpendicular to the steps can be hindered, so that the spreading is slower than on the step-free surface; and on the other hand, the spreading along the steps could be enhanced. We cannot distinguish between these two possibilities from our experiments. Butz and Wagner¹⁸ performed experiments for the spreading of Pd on W(110) with different step densities and found that the step density has no influence on the spreading length perpendicular to the steps, but the higher the step density the larger the spreading length along the steps. Therefore, they concluded that the spreading perpendicular to the steps is not hindered but the spreading along the steps is enhanced. This is supported by calculations by Natori and Godby.²⁸ They demonstrated that in a steady-state situation, which is present in the case of spreading by the "unrolling carpet" mechanism, only the Schwoebel barrier is effective and not the higher binding energies at ledge sites. This means that steps without the Schwoebel barrier do not hinder the spreading perpendicular to the step direction at all. The effective diffusion coefficient D_{eff} for diffusion perpendicular to the steps can be calculated after^{13,29}

$$D_{\text{eff}} = \frac{D_T D_S (w_T + w_S)}{D_T w_S + D_S w_T}. \quad (3)$$

In Eq. (3) D_T is the diffusion coefficient for diffusion over the terraces, D_S the diffusion coefficient for diffusion over the steps, w_T the mean terrace width and w_S the width of a step. The highest Schwoebel barrier observed so far is 0.2 eV.³⁰ If we take this value and assume w_T as 30 nm (corresponds to a miscut of 0.4°) and w_S as 3 Å, then D_{eff} for 820 K is $0.87D_T$. This is quite a small effect and cannot account alone for the observed ratio of spreading length along the steps: spreading length perpendicular to the steps of 10:1 (Fig. 2). So it seems probable that mainly an enhanced spreading along the steps causes the step related anisotropy.

Butz and Wagner¹⁸ developed an extension of the "unrolling carpet" model to describe the enhanced spreading along steps. They split the diffusion current into the current along the steps j_S and into the current across the terraces j_T . The currents are described by

$$j_T = D_T \frac{\partial c_T}{\partial X}$$

$$j_S = N D_S \frac{\partial c_S}{\partial X}. \quad (4)$$

In Eq. (4) D_S the diffusion coefficient for diffusion along steps, N the step density, and c_T and c_S are the concentrations on top of the first ML on terraces and at steps, respectively. For a fixed X the two concentrations are in thermal equilibrium with each other which means that

$$c_S = c_T e^{(E_S - E_T/kT)} \quad (5)$$

is valid with E_S being the binding energy for a ledge site and E_T the binding energy for a terrace site. Because the binding energy at ledge sites is higher than at terrace sites, for a fixed diffusion temperature the concentration at ledge sites is a certain factor higher than at terrace sites for every fixed X . This results in a higher concentration gradient along steps compared to the concentration gradient along terraces [Fig. 5(b)]. Therefore, j_S can be bigger than j_T even if $N D_S$ is smaller than D_T , as should be the case for typical mean terrace widths. The model of Butz and Wagner¹⁸ gives, for the relation between the two currents,

$$\frac{j_S}{j_T} = A_0 e^{\delta E/kT}, \quad \delta E = E_{dT} - E_{dS} + E_S - E_T \quad (6)$$

with E_{dT} (E_{dS}) the activation energy for diffusion over the terraces (along steps). A_0 is a temperature-independent factor depending on the geometry of the surface, especially on the step density. The higher the step density the larger is A_0 , i.e., the more important is the mass transport along steps. The energy δE , describing the temperature dependence of the influence of steps on the spreading anisotropy, should not be confused with the overall activation energy E , describing the temperature dependence of the spreading length. The term $E_{dT} - E_{dS}$ in δE originates from the different activation energies for diffusion along steps or across terraces, respectively. In most cases the activation energy for diffusion along steps will be higher than for terrace diffusion due to the higher

coordination at the ledge site. Therefore, this term would be negative. For some systems there is experimental evidence³¹ or theoretical prediction^{32–34} for diffusion along steps having a lower activation energy compared to terrace diffusion. In this case $E_{dT}-E_{dS}$ would be larger than zero. But even if this term is negative it will be outweighed by the second term. This term is positive because the binding energy at ledge sites is always higher than on terrace sites. $|E_S-E_T|$ should be larger than $|E_{dT}-E_{dS}|$ because activation energies for diffusion are in the range of 10–30 % of binding energies. Therefore, δE should always be positive. It is important to clarify that according to the model of Butz and Wagner presented here the mass transport along steps can dominate although the diffusion coefficient for diffusion along steps is smaller than for diffusion across terraces. The reason for this is that due to the differences in binding energy the concentration gradient, i.e., the driving force for mass transport, along steps is larger than on terraces.

Equation (6) can also explain the observed temperature dependence of the spreading anisotropy. The higher the diffusion temperature, the less important is mass transport along steps. The two diffusion currents are related to the observed spreading anisotropies in the following way: If j_T is much bigger than j_S , the anisotropy will be determined by the crystallographic structure in the diffusion zone. On the other hand, if the diffusion current along the steps is much bigger than the current across the terraces, the direction of fast spreading will be that of the step direction. This means that at higher diffusion temperatures the crystallographic structure tends to determine the anisotropy whereas steps have the strongest influence for low temperatures. We observe exactly that behavior in our experiments for the spreading of Co and Ni. Without making any assumption on the step density, we may say that

$$\delta E_{\text{Fe}} < \delta E_{\text{Co}} < \delta E_{\text{Ni}}. \quad (7)$$

We note that this is the first time that the crossover from step-controlled spreading anisotropy to an anisotropy determined by the crystallographic structure with increasing diffusion temperature as predicted by the model of Butz and Wagner has been observed experimentally.

For experimental reasons it is not feasible to study the spreading behavior of Ni and Co quantitatively in a temperature range where the crystallographic structure determines the anisotropy. However, in the temperature range where the spreading along the steps dominates, the spreading length along the steps should be proportional to the square root of the diffusion time and for the temperature dependence of the spreading length Eq. (2) should hold if $E = E_a + E_{dT}$ is replaced by $E = E_{dS} + E_a + E_T - E_S$.¹⁸ We find that our experimental data fulfill the predicted time dependence as well as the temperature dependence. In Table I the overall activation energies E are listed. The activation energies will be discussed below in comparison with the results for the Cu spreading.

For Cu we have observed different spreading anisotropies for the 1 and 2 ML zone, respectively. For the first ML the fast spreading direction is along the steps throughout the entire temperature range investigated (up to 820 K). This can be explained by the model discussed above. By comparison with Co we can conclude that δE_{Cu} is at least as big as

TABLE I. Overall activation energies for the spreading of Fe, Co, Ni and the first ML Cu as well as spreading lengths along the fast spreading direction at 820 K.

	Fe	Co	Ni	Cu (First ML)
E/eV	1.2 ± 0.1	0.9 ± 0.1	1.1 ± 0.2	0.7 ± 0.1
X_b after 24' at 820 K/ μm	$\leq 25 \pm 5$	158 ± 5	168 ± 5	367 ± 5

δE_{Co} . The second ML spreads fast along $\langle 100 \rangle$. Steps cannot be the reason for this fast spreading direction of the second ML so that probably the crystallographic structure of the 2 ML zone determines the anisotropy. Lilienkamp and co-workers³⁵ reported that 2 ML Cu on W(110) show a 1×15 superstructure. This corresponds to a distorted fcc(111) structure with pseudomorphism along $\langle 100 \rangle$ and an additional periodicity along $\langle 110 \rangle$. Due to surface buckling on an atomic scale this structure shows ‘‘channels’’ along $\langle 100 \rangle$. We think that this channel structure causes a fast spreading along $\langle 100 \rangle$ because the binding sites along $\langle 110 \rangle$ are not equivalent and it is, thus, probable that an atom faces an additional energy barrier if it tries to leave the channel.

The spreading of Cu along the steps can be described quantitatively by the same coupled equations as derived by Noro and co-workers²⁶ for the system Ag/Fe(110). In general, these equations cannot be solved, but Noro and co-workers reported that for a certain thickness of the initial Ag deposit the edge of the 2 ML zone does not move. In this case the spreading of the first ML can be described in the same way as discussed for the Co spreading with the edge of the second ML as a source for diffusing atoms. The leaving atoms are replaced by atoms from the three-dimensional islands formed on top of the second ML. For Cu one can also find a thickness for the initial dot so that the 2 ML edge does not move. This thickness is 4.5 ML. Our experimental data show the predicted correlation between the spreading length X_b and the diffusion time t (X_b proportional to \sqrt{t}). The overall activation energy for the spreading of the first ML Cu is listed in Table I.

Now the spreading behavior of the four metals investigated will be compared. For Fe the spreading length is much smaller than for Co, Ni, and the first ML Cu (Table I) along the fast direction. The comparison of the overall activation energies shows very similar values for Fe, Co, and Ni, but one has to take into account, that for Fe the mass transport occurs over the terraces whereas for the other three metals mass transport along the steps dominates. We think that the additional mass transport along the steps accounts for the larger spreading length for Co and Ni compared to Fe. For the first ML Cu we have the biggest spreading length, which corresponds well to the fact that we also observe the lowest overall activation energy. This low activation energy together with the mass transport along the steps accounts for the large spreading length for Cu.

For none of the investigated metals is it feasible to extract the individual contributing energies, e.g., E_{dT} , from the overall activation energy because none of them is independently known from experiment or from theory. All one can say is that the overall activation energies determined from our experiments are of the right order of magnitude. The

activation energies for diffusion are in the range of some tenth of an eV and the differences in binding energy between various sites should be up to 1 eV.^{4,32,33} Bond counting arguments similar to those used by Burton, Franck, and Cabrera³⁶ in their TKL model suggest that all binding energies, for instance, at a ledge site, and all activation energies, e.g., E_{dT} , scale with the binding energy for atoms in the second ML in the same way for Fe, Co, Ni, and Cu. This does not agree with our experimental findings for the following reasons: If the contributing single energies scale for each metal in the same way, then δE and the overall activation E should vary in the same manner between the different metals. Experimentally it is observed that the spreading of the first ML Cu has by far the smallest overall activation energy but the δE is at least as large as for the Co spreading. The second point is that the binding energies for Fe, Co, and Ni in the second ML are nearly the same, as can be concluded from TDS.^{8,9,10} This means, that the big differences in δE between the three metals, indicated by the large differences in influence of steps on the spreading behavior, cannot be explained by the assumption that the single energy contributions scale with the binding energy in the second ML. Obviously simple bond counting arguments cannot explain our experimental findings.

A factor that one has certainly to take into account is the influence of the substrate. For example, the substrate causes a strain in the metal overlayers. The pseudomorphic Fe ML is homogeneously strained by -9.4% (tensile strain) whereas the pseudomorphic ML for Co and Ni are inhomogeneously strained. The tensile strain along $\langle 110 \rangle$ is -3.6% (-2.8%) and along $\langle 100 \rangle$ 21.2% (20.7%) for Ni (Co). Diffusion on strained surfaces was theoretically investigated by Schroeder and Wolf³⁷ for (100) surfaces of fcc, bcc, and sc crystals. They found that strains of 5% significantly change the activation energies for diffusion on terraces. In general, tensile stress increases the energy barrier whereas compressive stress reduces the activation energy. How the strain affects the activation energy for diffusion along steps is not known so far. It seems possible that in our experiments the differences in the strain account for differences in the diffusion behavior between Fe on the one hand and Co and Ni on the other hand. We think that to fully understand the influence of the substrate on the single energy contributions to δE

and the overall activation energy E and to reproduce our experimental results one has to carry out a detailed theoretical investigation calculating a complete set of relevant binding and activation energies for each metal.

V. CONCLUSIONS

We have performed spreading experiments for Fe, Co, Ni, and Cu on W(110). Our results can be summarized as follows.

(a) For Fe, Co, and Ni one pseudomorphic ML spreads across the surface. This behavior can be explained by the “unrolling carpet” model. For Cu 1 and 2 ML spread out simultaneously. The different spreading behaviors for Fe, Co, and Ni on the one hand and Cu on the other reflect the different binding situations. For Fe, Co, and Ni layers on top of the first ML have the same binding energy whereas for Cu the second layer has a higher binding energy than the subsequent layers.

(b) For Fe the crystallographic structure in the diffusion zone determines the spreading anisotropy up to 1070 K, which results in fast spreading along $\langle 110 \rangle$. For Co the fast spreading direction is along the steps of the substrate up to 920 K. Above 1000 K the anisotropy is determined by the crystallographic structure in the diffusion zone (fast spreading direction along $\langle 110 \rangle$). For Ni the influence of steps is even more pronounced and can be clearly seen up to 1070 K. Higher diffusion temperatures were not investigated because then significant desorption of the diffusing material occurs.

(c) The anisotropy for the spreading of the first ML Cu is determined by steps. For the second ML the fast spreading direction is along $\langle 100 \rangle$, which is caused by the crystallographic structure of the Cu layer at a thickness of 2 ML.

(d) We have determined the overall activation energies for the spreading processes for Fe, Co, Ni, and Cu (Table I).

We have shown that the anisotropy caused by steps is superimposed onto the anisotropy due to the crystallographic structure. Which anisotropy dominates is temperature dependent, as predicted by the model of Butz and Wagner. We observed for the first time the predicted crossover from a step-controlled spreading anisotropy at low diffusion temperatures to an anisotropy determined by the crystallographic structure at high diffusion temperatures.

¹H. P. Bonze, in *Surface Diffusion on Metals*, Landolt-Börnstein, New Series, Group III, Vol. 26, Chap. 13, edited by H. Mehrer (Springer-Verlag, Berlin, 1990).

²R. Gomer, *Rep. Prog. Phys.* **53**, 917 (1990).

³T. T. Tsong, *Rep. Prog. Phys.* **51**, 759 (1988).

⁴G. L. Kellogg, *Surf. Sci. Rep.* **21**, 1 (1994).

⁵A. G. Naumovets and Yu. S. Vedula, *Surf. Sci. Rep.* **4**, 365 (1985).

⁶H. J. Elmers, J. Hauschild, H. Höche, U. Gradmann, H. Bethge, D. Heuer, and U. Köhler, *Phys. Rev. Lett.* **73**, 898 (1994).

⁷M. Hehn, K. Ounadjela, J. P. Bucher, F. Rousseaux, D. Deccanini, B. Bartenlian, and C. Chappert, *Science* **272**, 1782 (1996).

⁸P. J. Berlowitz, J.-W. He, and D. W. Goodman, *Surf. Sci.* **231**, 315 (1990).

⁹B. G. Johnson, P. J. Berlowitz, D. W. Goodman, and C. Bartholomew, *Surf. Sci.* **217**, 13 (1989).

¹⁰P. J. Berlowitz and D. W. Goodman, *Surf. Sci.* **187**, 463 (1987).

¹¹J. E. Whitten and R. Gomer, *Surf. Sci.* **316**, 1 (1994).

¹²E. Bauer, H. Poppa, G. Todd, and F. Bonczek, *J. Appl. Phys.* **45**, 5164 (1974).

¹³J. Crank, *The Mathematics of Diffusion* (Oxford University Press, New York, 1967).

¹⁴R. Butz and H. Wagner, *Surf. Sci.* **63**, 448 (1977).

¹⁵E. Suliga and M. Henzler, *J. Phys. C* **16**, 1543 (1983).

¹⁶R. Butz and H. Wagner, *Surf. Sci.* **87**, 69 (1979).

¹⁷U. Kürpick, G. Meister, and A. Goldmann, *Appl. Surf. Sci.* **89**, 383 (1995).

¹⁸R. Butz and H. Wagner, *Surf. Sci.* **87**, 85 (1979).

- ¹⁹R. Gomer and J. K. Hulm, *J. Chem. Phys.* **27**, 1363 (1957).
- ²⁰U. Gradmann and G. Waller, *Surf. Sci.* **116**, 539 (1982).
- ²¹H. J. Elmers, J. Hauschild, H. Fritzsche, G. Liu, U. Gradmann, and U. Köhler, *Phys. Rev. Lett.* **75**, 2031 (1995).
- ²²H. Knoppe and E. Bauer, *Phys. Rev. B* **48**, 1794 (1993).
- ²³J. Kolaczkiwicz and E. Bauer, *Surf. Sci.* **144**, 495 (1984).
- ²⁴C. Koziol, G. Lilienkamp, and E. Bauer, *Phys. Rev. B* **41**, 3364 (1990).
- ²⁵J. Kolaczkiwicz and E. Bauer, *Surf. Sci.* **175**, 508 (1986).
- ²⁶H. Noro, R. Persaud, and J. A. Venables, *Surf. Sci.* **357/358**, 879 (1996).
- ²⁷R. A. Johnson and P. J. White, *Phys. Rev. B* **7**, 4016 (1973); T. T. Tsong, *ibid.* **7**, 4018 (1973).
- ²⁸A. Natori and R. W. Godby, *Phys. Rev. B* **47**, 15 816 (1993).
- ²⁹N. Y. Wu, H. Yasunaga, and A. Natori, *Surf. Sci.* **242**, 191 (1991).
- ³⁰S. C. Wang and T. T. Tsong, *Surf. Sci.* **121**, 85 (1982).
- ³¹C. L. Chen and T. T. Tsong, *Phys. Rev. B* **47**, 15 852 (1993).
- ³²M. Karimi, T. Tomkowski, G. Vidiali, and O. Bihan, *Phys. Rev. B* **52**, 5364 (1995).
- ³³C. L. Liu and J. B. Adams, *Surf. Sci.* **264**, 262 (1992).
- ³⁴B. D. Yu and M. Scheffler, *Phys. Rev. B* **55**, 13 916 (1997).
- ³⁵G. Lilienkamp, C. Koziol, and E. Bauer, *Surf. Sci.* **226**, 358 (1990).
- ³⁶W. K. Burton, N. Cabrera, and F. C. Frank, *Philos. Trans. R. Soc. London, Ser. A* **243**, 299 (1951).
- ³⁷M. Schroeder and D. E. Wolf, *Surf. Sci.* **375**, 129 (1997).